RESEARCH ARTICLE

Investigation of process parameters of electrohydrodynamic jetting for 3D printed PCL fibrous scaffolds with complex geometries

Hui Wang[1], Sanjairaj Vijayavenkataraman[2], Yang Wu[2], Zhen Shu[1], Jie Sun[1] and Jerry Fuh Ying Hsi[1,2*]

[1] NUS Suzhou Research Institute (NUSRI), No. 377 Linquan Street, Dushu Lake Science and Education Innovation District, Suzhou Industrial Park, Suzhou, Jiangsu, China 215123

[2] Department of Mechanical Engineering, National University of Singapore, 9 Engineering Drive 1, Singapore 117575

Abstract: Tissue engineering is a promising technology in the field of regenerative medicine with its potential to create tissues *de novo*. Though there has been a good progress in this field so far, there still exists the challenge of providing a 3D micro-architecture to the artificial tissue construct, to mimic the native cell or tissue environment. Both 3D printing and 3D bioprinting are looked upon as an excellent solution due to their capabilities of mimicking the native tissue architecture layer-by-layer with high precision and appreciable resolution. Electrohydrodynamic jetting (E-jetting) is one type of 3D printing, in which, a high electric voltage is applied between the extruding nozzle and the substrate in order to print highly controlled fibres. In this study, an E-jetting system was developed in-house for the purpose of 3D printing of fibrous scaffolds. The effect of various E-jetting parameters, namely the supply voltage, solution concentration, nozzle-to-substrate distance, stage (printing) speed and solution dispensing feed rate on the diameter of printed fibres were studied at the first stage. Optimized parameters were then used to print Polycaprolactone (PCL) scaffolds of highly complex geometries, i.e., semi-lunar and spiral geometries, with the aim of demonstrating the flexibility and capability of the system to fabricate complex geometry scaffolds and biomimic the complex 3D micro-architecture of native tissue environment. The spiral geometry is expected to result in better cell migration during cell culture and tissue maturation.

Keywords: 3D printing, PCL scaffolds, E-jet printing

*Correspondence to: Jerry Fuh Ying Hsi, Department of Mechanical Engineering, National University of Singapore, 9 Engineering Drive 1, Singapore 117575; Email: jerry.fuh@nus.edu.sg

Received: October 26, 2015; **Accepted:** November 24, 2015; **Published Online:** January 5, 2016

Citation: Wang H, Vijayavenkataraman S, Wu Y, *et al*., 2016, Investigation of process parameters of electrohydrodynamic jetting for 3D printed PCL fibrous scaffolds with complex geometries. *International Journal of Bioprinting*, vol.2(1): 63–71. http://dx.doi.org/10.18063/IJB.2016.01.005.

1. Introduction

Scaffolds have a significant role in tissue engineering. In brief, cells are cultured *in vitro* on a scaffold and allowed to migrate, proliferate and differentiate, which eventually attached to the scaffold and developed into a tissue. Most of the times, the engineered tissue is incubated in a bioreactor to facilitate maturation. The structure and properties of the final engineered tissue predominantly depends on the material, structure and properties of the scaffold. Many requirements are expected in order for scaffolds

to be successful in engineering a tissue[1–2], namely (i) scaffold should biomimic the native tissue environment as close as possible, (ii) material selection, should be biocompatible and biodegradable, (iii) appropriate surface chemistry to promote cell attachment, proliferation and differentiation, (iv) adequate mechanical properties, and (v) fabrication flexibility to have a variety of shapes and sizes. The utmost challenge with the current tissue engineering techniques is imitation of the native tissue environment. Traditional tissue engineering methods use 2D materials or scaffolds for cell culture and tissue construction. The main drawback of 2D substrate is that it fails to provide the cell with its native architecture. Most importantly, native tissue micro-architecture is highly complex and highly oriented due to its 3D environment. Obviously, when a 3D environment is provided rather than 2D or 2.5D, the cells grow, proliferate and differentiate closer to the native tissue[3–5]. There are several techniques to create a3D environment, such as solvent-casting particulate-leeching, gas foaming, phase separation, melt moulding, solution casting, freeze drying and emulsion freeze drying, however, they suffer from the drawback of producing only a foam structure, and not a highly controlled porous 3D micro-architecture, which leads to several other problems[6]. Though microscale fabrication technologies like soft lithography were able to create a microscale resolution scaffold[7–8], they also suffer from several limitations associated with inflexibility in fabricating complex geometries and the optimization of scaffold architecture[9]. Electrospinning is looked at as an alternate technology to fabricate nanofibrous scaffolds for tissue engineering applications[10–14] and shows a considerable progress with several reports portraying its successfulness. Nonetheless, electrospinning technology suffers from the limitation of randomly oriented fibres and inability to fabricate a controlled uniformly porous scaffolds. 3D printing is currently seen as the potential solution to fabricate layer by layer, controlled 3D porous scaffolds[6,15–19]. A new term known as 3D bioprinting has emerged recently and researchers are working towards the realization of printing functional human organs with this novel technology. An *et al*.[20] reviewed vastly on various state-of-the-art 3D printing technologies for tissue engineering applications, limitations of the current technologies and the possible future improvements. Electrohydrodynamic Jetting, which is also known as EHD-Jetting or E-jetting is one type of bioprinting technology. E-jetting has the same working principle as Electrospinning technique which is widely used to fabricate controlled porous scaffolds for tissue engineering applications[21–26]. Various studies were made on the effect of Electrospinning parameters on the electrospun fibres[27–28]. Subsequently, the most important parameters that have been identified were namely, the volumetric charge density, distance from nozzle to collector, initial jet/orifice radius, relaxation time, and viscosity[29]. Numerous novel and hybrid techniques of Electrospinning were developed in order to overcome the limitation of non-orientated random fibres from the Electrospinning process. Bu *et al*.[30] developed a mechano-electrospinning technique for fabricating oriented nanofibres and the controlled parameter was the moving speed of the substrate. Chanthakulchan *et al*.[31] developed an Electrospinning-based rapid prototyping method for fabrication of patterned scaffolds but only achieved a certain level, due to the challenges of controlling the vibration. Auyson *et al*.[32] studied the effect of various parameters of the hybrid Electrospinning / Fused Depositio Modelling (FDM) on the fabricated scaffold and concluded that two most important parameters to get a continuous jet are the voltage applied and the standoff distance between the nozzle and the substrate. On the other hand, a low voltage near-field Electrospinning method reported by Bisht *et al*.[33] was able to pattern nanofibres continuously on both 2D and 3D substrates, respectively. Besides that, other vital parameters were namely, the viscosity and elasticity of the polymer ink[34].

In this study, an E-jetting setup was built in-house in order to fabricate 3D scaffolds out of PCL material. PCL material is widely used as a biomaterial for scaffolds which possess extremely good mechanical properties. The structure of the printed scaffold depends on two important elements namely, the fibre diameter and the pore size. The parameters of the E-jetting system, i.e. the supply voltage, solution concentration, nozzle-to-substrate distance, stage (printing) speed and solution dispensing feed rate greatly influences the fibre diameter of the printed structure. Briefly, the relation between these parameters and the fibre diameter were discussed in this work. Parameters were optimized and scaffolds of complex geometries i.e. semi-lunar and spiral shapes have been successfully printed.

2. Experimental Section

2.1 Materials

Acetate (Aladdin A116171, electronic grade, >99.7%)

which is commonly referred to acetic acid was used as the solvent. Polycaprolactone (PCL) pellets with an average molecular weight of 80 kDa (Polycaprolactone, Scientific Polymer Products Inc, Ontario, NY) was used as the solute biomaterial. PCL pellets were put in the acetic acid solution (50%, 60%, 70%, 80% and 90%) (w/v) and sonicated by using an ultrasonic sonicator at 30°C and 40 kHz for 3 hours. Then, the mixture was stirred well and re-sonicated for another 1.5 hours in order to obtain a homogeneous solution. The solution was left at room temperature for a while before unloaded it into the syringe for E-jetting purpose. Polished silicon wafers with the diameter of 100 mm were used as substrates.

2.2 Experimental Setup

An E-jetting system was built in-house for the purpose of fabrication of scaffolds. The schematic diagram of the experimental setup and the actual system are shown in Figure 1 and Figure 2, respectively. The main components of the system are namely, the high voltage power source, a high precision XYZT stage along with the controller, a syringe pump and a computer. The software for stage control, connecting tubes, syringes and needles are other components. A 13 mm internal diameter syringe and 0.5 mm internal diameter needle were used in all the experimental trials. The high precision stage, purchased from Aerotech Company (Pittsburgh, PA, USA) was driven by linear motors. The X and Y axis has the travel distance of up to 150 mm and can be precisely controlled up to 3 μm, while the Z axis has the travel distance of 50 mm and can be precisely controlled up to 5 μm. Ensemble

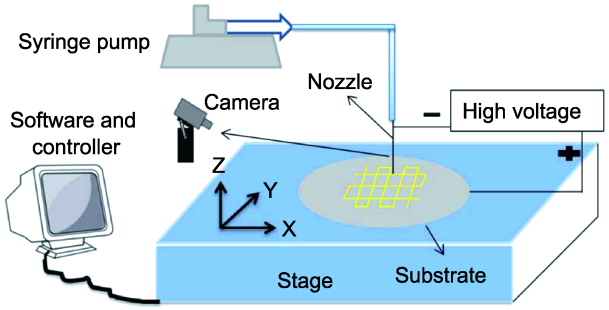

Figure 1. Conceptual diagram of E-jetting system.

IDE is the software that controls the movement of the XYZT stage through a communication interface, which also gives the real-time position and velocity information for effective monitoring and control.

The working principle is based on the balance between the electrostatic force and the combined surface tension and viscoelastic force of the liquid. A high voltage (DC) is applied between the nozzle and the substrate, typically in the order of 2–3 kV. The surface tension force of the liquid at the nozzle tip was overcome by the electrostatic force between the nozzle and substrate, hence forcing the solution to come out of the nozzle and printed onto the substrate. The whole process happens in two stages. The first stage was the formation of the Taylor cone at the apex of the conical meniscus, due to which the electric field stretches the liquid. Then it progresses to the second stage of Rayleigh-Plateau instability. As the electric field force increases, Rayleigh-Plateau instability becomes larger than the combined surface tension and viscoelastic force, while a jet of liquid is formed and ejected continuously onto the substrate. The substrate

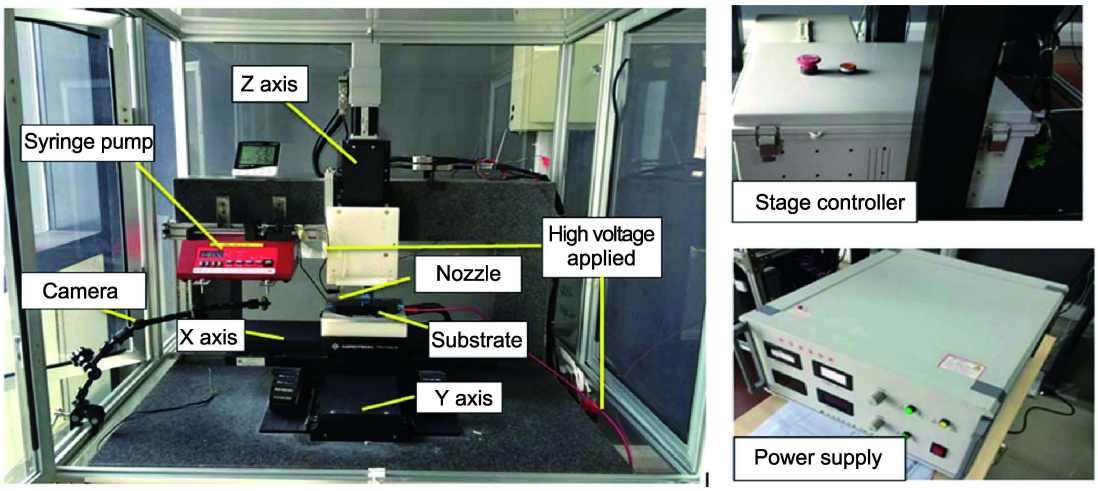

Figure 2. In-house E-jetting system.

was placed on the XYZT stage and moved in accordance to the computer program pertaining to the desired geometry, pore size and number of layers. A square-mesh pattern is used for the optimization studies of various parameters and its effects on the fibre diameter. The traverse path of square-mesh scaffolds is shown in Figure 3.

2.3 Characterization of Fibrous Scaffolds

The morphology of fibre was analysed under an Optical Microscope (OLYMPUS, BX51M) and FESEM (FEI Quanta 250 FEG, FEI Inc, OR, USA) at an accelerating voltage of 15 kV. Acceleration voltage is the voltage in which the electrons are accelerated down the SEM column. In other words, it is the highest voltage applied to the filament. The higher the accelerating voltage, the faster the electrons travel down the column and the more penetrating power they have, reducing spherical abberation of the system and thereby increasing the resolution. The diameter of the fibre was measured both using the optimal microscope images (MShot Digital Imaging System software) and FESEM. Six measurements were made and the average value was calculated. The images from optical microscope and SEM are shown in Figure 4. The sample size for each data point for all the experiments was three whereas the standard deviation (SD) was less than 20 μm. In fact, most of the data points had a SD of 2–5 μm.

3. Results and Discussion

3.1 Effect of Stage Speed on Fibre Diameter

The effect of varying stage speed on fibre diameter is shown in Figure 5. Stage speed is varied from 10 mm/s to 140 mm/s, while all other parameters are kept constant (Fd = 6 μL/min, D = 3 mm, V = 3 kV), at two different solution concentrations (C) viz. 50% and 70% w/v. As expected, the size of the fibre diameter decreased with the increment of stage speed. This is due to the fact that at higher speed, the duration of e-jetting at a particular point of substrate have lessened and the fibre's diameter was also reduced naturally. However, at very high speeds, discontinuous fibres resulted. This might be because of the fact that the frictional force between the jetted fibre and the substrate increases greatly at very high speeds, which at a certain critical value exceeds the viscoelastic force and hence results in discontinuous fibres. In other words, when the stage speed was increased to more than 160 mm/s, the traction force caused by the adhesion in-between the nozzle and substrate could exceed the viscoelastic force of the PCL fibre, thus resulting in the formation of discontinuous fibres

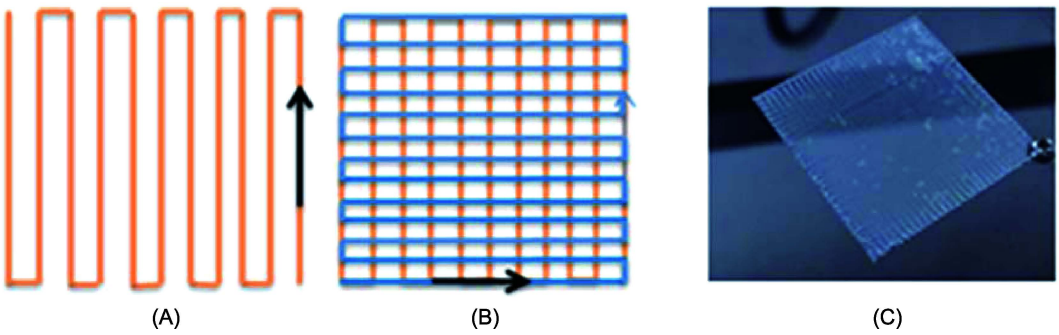

Figure 3. Traverse path of the square-mesh scaffold, **(A)** first layer **(B)** second layer **(C)** E-jetted square- mesh PCL scaffold, 40 x 40 mm, pore size of 0.5 x 0.5 mm and fibre diameter of 100 μm.

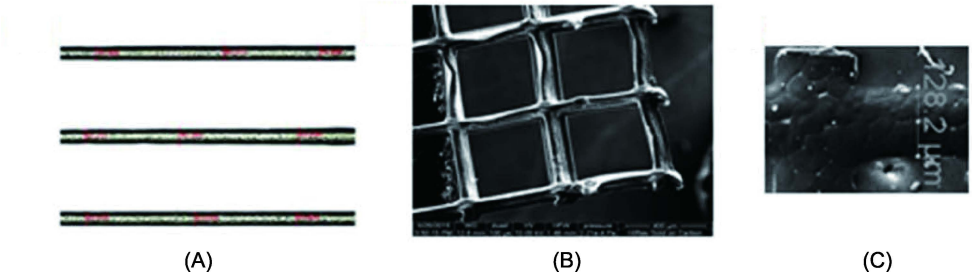

Figure 4. Characterization of fibre through **(A)** Optical Microscope and **(B)** SEM. **(C)** A closer view of the SEM measurement.

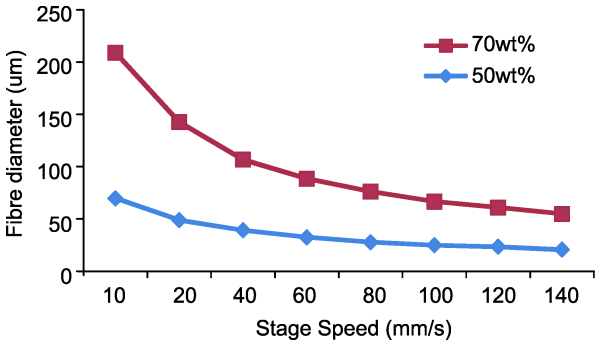

Figure 5. Effect of stage speed on fibre diameter.

or no fibre being attached onto the substrate. On top of that, the effect of stage speed on fibre diameter was found to be different at various solution concentrations. With increase in concentration the fibre diameter is larger, at the same stage speed . As seen from Figure 5, at a particular stage speed, the fibre diameter of 70% w/v solution is much higher than that of 50% w/v solution. On an average, the difference is more than 40%, which is predominantly due to the increase in the viscoelastic force, with increase in the concentration. The effect was more pronounced at lower speeds and the differences were narrowed down slowly as the stage speed increases, which apparently prove the same fact.

3.2 Effect of Solution Feed Rate on Fibre Diameter

The feed rate at which the solution was delivered by the syringe pump to the nozzle and onto the substrate plays a significant role in determining the final fibre diameter. Figure 6 shows the relationship between the solution feed rate and fibre diameter. The solution feed rate was varied from 4 to 20 µL/min, while the other parameters were kept constant (D = 2.5 mm, V = 3 kV and S = 150 mm/s). The study was conducted in three different solution concentrations (60%, 70% and 90%) (w/v). The fibre diameter increased with increase in solution feed rate, as expected. At the same stage speed and voltage, when the feed rate is increased, the amount of solution that is e-jetted out of the nozzle per unit of time will also increase, thereby resulting in deposition of an increased volume of solution on the substrate and hence, the fibre diameter also increases. Also, at the same feed rate, solutions with higher concentration resulted in greater fibre diameter than the solution with lower concentration, which is due to the dominant viscoelastic force as discussed in the previous section. One important observation to make is that at very high concentration (90% w/v), the effect of solution feed rate is much less pronounced compared to the low concentration solutions. To put it in other words, for the same range of feed rate variation (4–20 µL/min), the variation range of fibre diameter is larger in low concentration solutions (50 µm to as large as 200 µm), whereas the fibre diameter range is considerably lesser in high concentration solution (100 µm to 140 µm only). This is attributed to the reason that the viscoelastic force due to the higher solution concentration is so dominant that the effect of increased feed rate becomes very less.

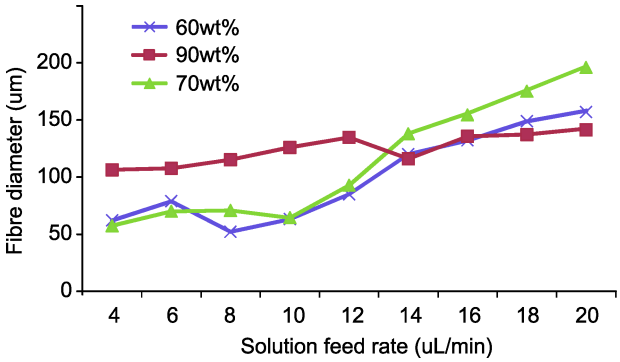

Figure 6. Effect of solution feed rate on fibre diameter.

3.3 Effect of Supply Voltage on Fibre Diameter

Supply voltage is a very important parameter in the E-jetting process, not only for the integrity of the fibre structure but also a safety concern. Too high values may result in sparking, eventually leading to greater safety risks. It is important to know the effect of supply voltage on fibre diameter so as to not exceed a certain value for safety reasons. The relationship between the supply voltage and the fibre diameter is shown in Figure 7. Voltage is varied from 2 kV to 3.5 kV, in small steps, with all other parameters constant (D = 2.5 mm, Fd = 10µL/min, S = 150 mm/s) and at three different solution concentrations (60% w/v, 70% w/v and 80% w/v). Voltage values below 2 kV resulted in discontinuous jet formations because of the inability of the electric field force to overcome the surface tension and viscoelastic force of the solution. The relationship is not well established and the trend is not regular. However, two regions could be identified. In the first region, at lower voltages, a small change in voltage resulted in a major change in the fibre diameter, For instance, at a solution concentration of 60% w/v, when the voltage is increased from 2 to 2.4 kV, the diameter increased from 20 to 100 µm and at solution concentration of 70%

w/v, when the voltage is increased from 2 to 2.4 kV, the diameter increased from 55 to 95 µm. This is followed by the second region, where the effect of increased voltage has less pronounced effect on the fibre diameter. This may be due to the reason that in region one, there lies the transition point at which the electric field force reaches a critical value and when it exceeds the combined effect of surface tension and viscoelastic forces. However, at a higher solution concentration, the trend looks murky and no stable pattern and the effect is also less pronounced, due to the dominant viscoelastic force. This may also be attributed to the complex interaction between the supply voltage and nozzle-to-substrate distance, which goes hand in hand.

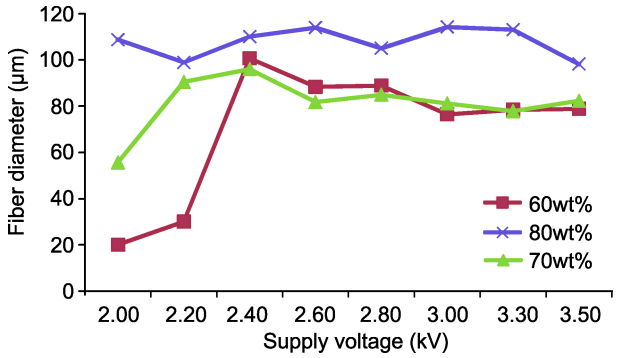

Figure 7. Effect of supply voltage on fibre diameter.

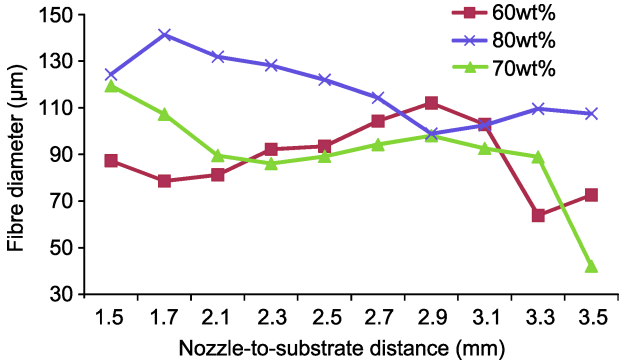

Figure 8. Effect of nozzle-to-substrate distance on fibre diameter.

3.4 Effect of Nozzle-to-substrate Distance on Fibre Diameter

Another important parameter which plays a significant role in the E-jetting process is the gap between the nozzle and the substrate. This parameter works relative to the supply voltage, i.e., if the gap is very small, applying a higher voltage will result in sparking and if the gap is very large, a very high voltage is required to overcome the surface tension and viscoelastic forces of the solution. The relationship between the nozzle-to-substrate distance and the fibre diameter is shown in Figure 8. Nozzle-to-substrate distance is varied from 1.5 to 3.5 mm, in small steps, with all other parameters constant (V = 2.5 kV, Fd = 10µL/min, S = 150 mm/s) and at three different solution concentrations (60% w/v, 70% w/v and 80% w/v). Values below 1.5 mm resulted in sparking. The observed relationship has no regular trend. But certain important observations can be made. While at lower values of gap, the fibre diameter increases at some concentrations and decreases at some other concentrations when the gap is increased, eventually there is a plateau region, where the fibre diameter doesn't vary much and is stable. After a certain higher value of nozzle-to-substrate distance, the fibre diameter tends to decrease drastically. This is due to the reason that when the gap is larger, at the same supply voltage, the electric field force at the nozzle tip reduces greatly and hence unable to overcome the surface tension and viscoelastic forces and also the fibres were not very stable and discontinuous. The trend is a bit different at very high solution concentration; in the plateau (middle) region where for other lower concentrations (60% w/v, 70% w/v) the fibre diameter does not vary much, it decreases in the higher concentration solution (80% w/v), again due to the dominant viscoelastic force.

3.5 3D Printing of PCL Scaffolds with Complex Geometries

From the parametric study, the E-jetting process was optimized and range for each parameter is obtained so as to get stable, continuous E-jetting fibres. The concentration of the PCL solution was fixed at 70% w/v, stage speed at 150 mm/s, supply voltage 2.5 to 3 kV, solution feed rate 4-10µL/min and nozzle -to-substrate distance 2.5 or 3 mm for all the subsequent experimental trials. Scaffolds of different geometries, with complex architecture were printed. Semi-lunar or curved scaffolds are printed as shown in Figure 9. This geometry is necessary for reconstruction of soft tissues especially the knee meniscus[35]. The E-jetting parameters were C = 70%, Fd = 8uL/min, V = 3 kV, S = 150 mm/s and D = 2.5 mm. Several trials were made and the fibre diameter measured was 90 ± 5 µm. A novel spiral scaffold was also printed as shown in Figure 10 for the first time. The E-jetting parameters were, for Figure 10C, C = 70%, Fd = 6 uL/min, V = 2.5 kV, S = 100 mm/s and D = 3 mm, and for Figure 10D, C = 70%, Fd = 0.4 uL/min, V = 2.55 kV, S = 100 mm/s and

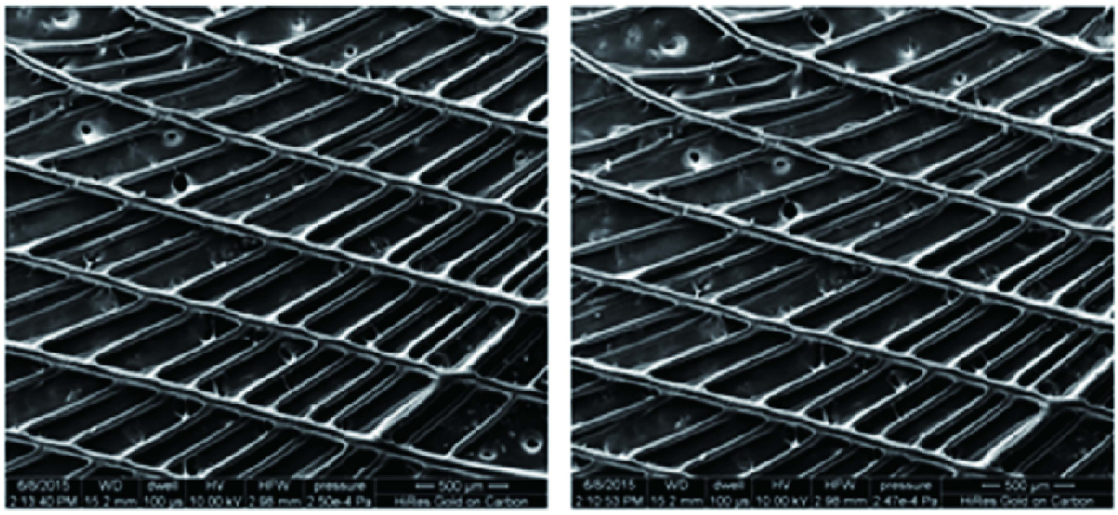

Figure 9. SEM Images of semi-lunar PCL scaffolds.

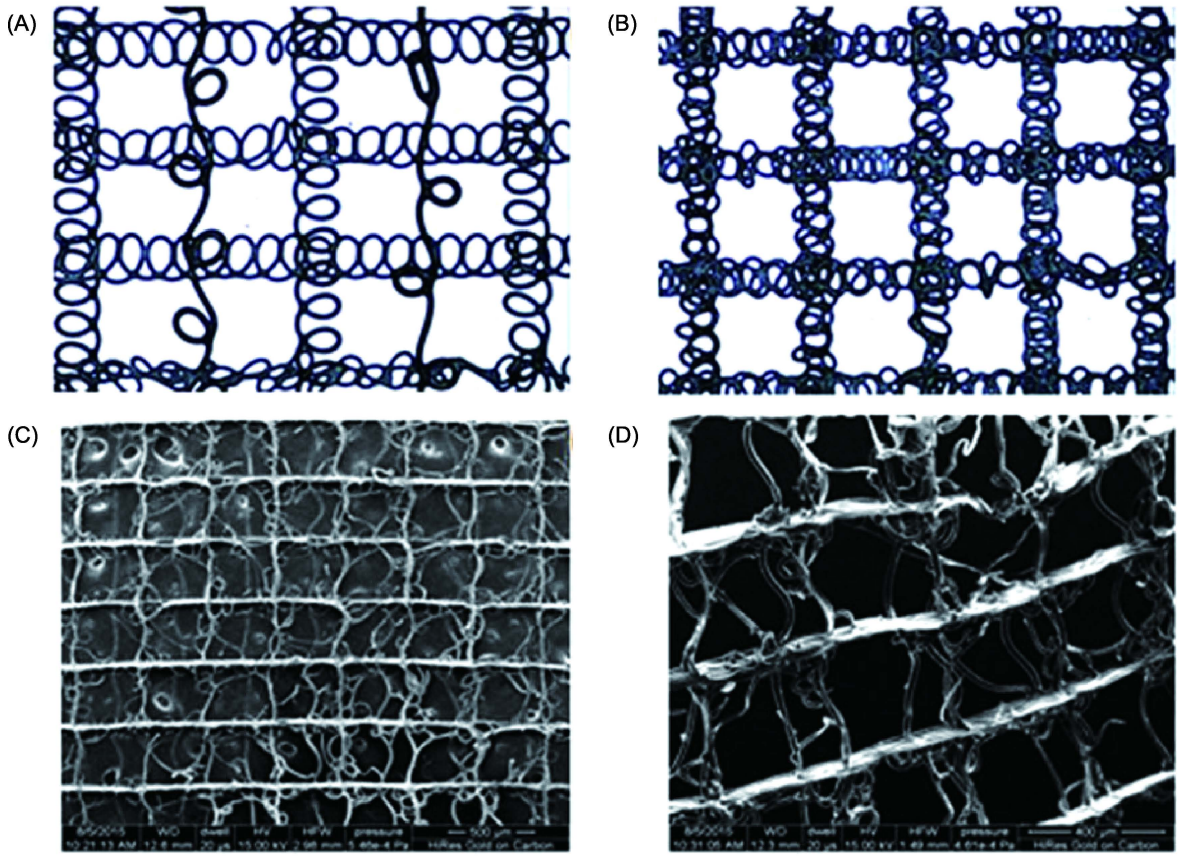

Figure 10. (A) & **(B)** Conceptual images of spiral scaffold. **(C)** & **(D)** SEM Images of spiral PCL scaffolds.

D = 3 mm. Different types of cells show different proliferation responses to the environment. Spiral scaffolds may be suitable for tissue engineering of soft tissues, with the spiral design improving the cell migration and formation of cell-cell junctions.

4. Conclusion

Development of the field of tissue engineering and successful clinical translation of this technology depends on how closely the engineered tissue biomimic

the native tissue architecture. 3D printing of scaffolds for tissue engineering and 3D Bioprinting are relatively new technologies which have the potential to meet this requirement. In this study, E-jetting process is studied in detail and the effect of various parameters on the printed fibre diameter analysed, pertaining to PCL biomaterial. The relationship between these parameters, in combination, is complex. Hence, a detailed parametric study has to be performed for finding the optimum parameters of E-jetting to print stable, regular, continuous fibres and hence scaffolds with good structural and spatial properties. In fact, the greatest advantage of this technology is the patterning and orientation of fibres in a controlled manner in desired architecture. The complex geometries like semi-lunar and spiral shaped scaffolds are printed using this technique, which will be very useful for certain complex soft tissues in body like the knee meniscus or tendon. These different complex shapes are also expected to influence the cell proliferation positively, in terms of better cell migration within the scaffold and formation of cell-cell junctions, which has to be validated by future in vitro studies. Development of the field of tissue engineering and successful clinical translation of this technology depends on how closely the engineered tissue biomimic the native tissue architecture. Both 3D printing of scaffolds for tissue engineering and 3D bioprinting are relatively new technologies which have the potential to meet this requirement. In this study, E-jetting process is studied in detail and the effect of various parameters on the printed fibre diameter analyzed, pertaining to PCL biomaterial. The relationship between these parameters, in combination, is complex. Hence, a detailed parametric study has to be performed for finding the optimum parameters of E-jetting process to print stable, regular, continuous fibres and hence scaffolds with good structural and spatial properties. In fact, the greatest advantage of this technology is the patterning and orientation of fibres in a controlled manner in desired architecture. The complex geometries like semi-lunar and spiral shaped scaffolds are printed using this technique, which will be very useful for certain complex soft tissues in body like the knee meniscus or tendon. These different complex shapes are also expected to influence the cell proliferation positively, in terms of better cell migration within the scaffold and formation of cell-cell junctions, which has to be validated by future *in vitro* studies.

Conflict of Interest and Funding

No conflict of interest was reported by the authors.

References

1. Hutmacher D W, 2001, Scaffold design and fabrication technologies for engineering tissues — state of the art and future perspectives. *Journal of Biomaterials Science, Polymer Edition*, vol.12(1): 107–124. http://dx.doi.org/10.1163/156856201744489
2. Hutmacher D W, Schantz T, Zein I, *et al*., 2001, Mechanical properties and cell cultural response of polycaprolactone scaffolds designed and fabricated via fused deposition modelling. *Journal of Biomedical Materials Research*, vol.55(2): 203–216. http://dx.doi.org/10.1002/1097-4636(200105)55:23.0.CO;2-7
3. Cukierman E, Pankov R, Stevens D R, *et al*., 2001, Taking cell-matrix adhesions to the third dimension. *Science*, vol.294(5547): 1708–1712. http://dx.doi.org/10.1126/science.1064829
4. Cukierman E, Pankov R and Yamada K M, 2002, Cell interactions with three-dimensional matrices. *Current Opinion in Cell Biology*, vol.14(5): 633–640. http://dx.doi.org/10.1016/S0955-0674(02)00364-2
5. Edelman D B and Keefer E W, 2005, A cultural renaissance: *In vitro* cell biology embraces three-dimensional context. *Experimental Neurology*, vol.192(1): 1–6. http://dx.doi.org/10.1016/j.expneurol.2004.10.005
6. Sachlos E and Czernuszka J T, 2003, Making tissue engineering scaffold work: Review on the application of SFF technology to the production of tissue engineering scaffolds. *European Cells and Materials*, vol.5(1): 29–40.
7. Whitesides G M, Ostuni E, Takayama S, *et al*., 2001, Soft lithography in biology and biochemistry. *Annual Review of Biomedical Engineering*, vol.3(1): 335–373. http://dx.doi.org/10.1146/annurev.bioeng.3.1.335
8. Walker G M, Zeringue H C and Beebe D J, 2004, Microenvironment design considerations for cellular scale studies. *Lab on a Chip*, vol.4(2): 91–97. http://dx.doi.org/10.1039/b311214d
9. Khademhosseini A, Langer R, Borenstein J, *et al*., 2006, Microscale technologies for tissue engineering and biology. *Proceedings of the National Academy of Sciences of the United States of America*, vol.103(8): 2480–2487. http://dx.doi.org/10.1073/pnas.0507681102
10. Lannutti J, Reneker D, Ma T, *et al*., 2007, Electrospinning for tissue engineering scaffolds. *Materials Science and Engineering: C*, vol.27(3): 504–509. http://dx.doi.org/10.1016/j.msec.2006.05.019
11. Agarwal S, Wendorff J H and Greiner A, 2009, Progress in the field of electrospinning for tissue engineering applications. *Advanced Materials*, vol.21(32–33): 3343–3351. http://dx.doi.org/10.1002/adma.200803092

12. Li W J, Laurencin C T, Caterson E J, *et al*., 2002, Electrospun nanofibrous structure: A novel scaffold for tissue engineering. *Journal of Biomedical Materials Research*, vol.60(4): 613–621. http://dx.doi.org/10.1002/jbm.10167
13. Sill T J and von Recum H A, 2008, Electrospinning: Applications in drug delivery and tissue engineering. *Biomaterials*, vol.29(13): 1989–2006. http://dx.doi.org/10.1016/j.biomaterials.2008.01.011
14. Yang F, Murugan R, Wang S, *et al*., 2005, Electrospinning of nano/micro scale poly (L-lactic acid) aligned fibers and their potential in neural tissue engineering. *Biomaterials*, vol.26(15): 2603–2610. http://dx.doi.org/10.1016/j.biomaterials.2004.06.051
15. Richards D J, Tan Y, Jia J, *et al*., 2013, 3D printing for tissue engineering. *Israel Journal of Chemistry*, vol.53(9–10): 805–814. http://dx.doi.org/10.1002/ijch.201300086
16. Mironov V, Boland T, Trusk T, *et al*., 2003, Organ printing: Computer-aided jet-based 3D tissue engineering. *Trends in Biotechnology*, vol.21(4): 157–161. http://dx.doi.org/0.1016/S0167-7799(03)00033-7
17. Hollister S J, 2005, Porous scaffold design for tissue engineering. *Nature Materials*, vol.4(7): 518–524. http://dx.doi.org/10.1038/nmat1421
18. Boland T, Xu T, Damon B, *et al*., 2006, Application of inkjet printing to tissue engineering. *Biotechnology Journal*, vol.1(9): 910–917. http://dx.doi.org/10.1002/biot.200600081
19. Yeong W Y, Chua C K, Leong K F, *et al*., 2004, Rapid prototyping in tissue engineering: Challenges and potential. *Trends in Biotechnology*, vol.22(12): 643–652. http://dx.doi.org/10.1016/j.tibtech.2004.10.004
20. An J, Teoh J E M, Suntornnond R, *et al*., 2015, Design and 3D printing of scaffolds and tissues. *Engineering*, vol.1(2), 261–268. http://dx.doi.org/10.15302/J-ENG-2015061
21. Gupta A, Seifalian A M, Ahmad Z, *et al*., 2007, Novel electrohydrodynamic printing of nanocomposite biopolymer scaffolds. *Journal of Bioactive and Compatible Polymers*, vol.22(3), 265–280. http://dx.doi.org/10.1177/0883911507078268
22. Wei C and Dong J, 2013, Direct fabrication of high-resolution three-dimensional polymeric scaffolds using electrohydrodynamic hot jet plotting. *Journal of Micromechanics and Microengineering*, vol.23(2): 025017. http://dx.doi.org/10.1088/0960-1317/23/2/025017
23. Ahmad Z, Rasekh M and Edirisinghe M, 2010, Electrohydrodynamic direct writing of biomedical polymers and composites. *Macromolecular Materials and Engineering*, vol.295(4): 315–319. http://dx.doi.org/10.1002/mame.200900396
24. Li J L, Cai Y L, Guo Y L, *et al*., 2014, Fabrication of three-dimensional porous scaffolds with controlled filament orientation and large pore size via an improved E-jetting technique. *Journal of Biomedical Materials Research Part B: Applied Biomaterials*, vol.102(4): 651–658. http://dx.doi.org/10.1002/jbm.b.33043
25. Gasperini L, Maniglio D, Motta A, *et al*., 2014, An electrohydrodynamic bioprinter for alginate hydrogels containing living cells. *Tissue Engineering Part C: Methods*, vol.21(2): 123–132. http://dx.doi.org/10.1089/ten.TEC.2014.0149
26. Cai Y, Li J L, Poh C K, *et al*., 2013, Collagen grafted 3D polycaprolactone scaffolds for enhanced cartilage regeneration. *Journal of Materials Chemistry B*, vol.1(43): 5971–5976. http://dx.doi.org/0.1039/C3TB20680G
27. Doshi J and Reneker D H, 1993, Electrospinning process and applications of electrospun fibers, In *Industry Applications Society Annual Meeting, Conference Record of the 1993 IEEE*: 1698–1703.
28. Mitchell G R, Ahn K H and Davis F J, 2011, The potential of electrospinning in rapid manufacturing processes. *Virtual and Physical Prototyping*, vol.6(2): 63–77. http://dx.doi.org/10.1080/17452759.2011.590387
29. Thompson C J, Chase G G, Yarin A L, *et al*., 2007, Effects of parameters on nanofiber diameter determined from electrospinning model. *Polymer*, vol.48(23): 6913–6922. http://dx.doi.org/10.1016/j.polymer.2007.09.017
30. Bu N, Huang Y, Wang X, *et al*., 2012, Continuously tunable and oriented nanofiber direct-written by mechano-electrospinning. *Materials and Manufacturing Processes*, vol.27(12): 1318–1323. http://dx.doi.org/10.1080/10426914.2012.700145
31. Chanthakulchan A, Koomsap P, Auyson K, *et al*., 2015, Development of an electrospinning-based rapid prototyping for scaffold fabrication. *Rapid Prototyping Journal*, vol.21(3): 329–339. http://dx.doi.org/10.1108/RPJ-11-2013-0119
32. Auyson K, Koomsap P, Chanthakulchan A, *et al*., 2013, Investigation of applying electrospinning in fused deposition modeling for scaffold fabrication. In High Value Manufacturing: Advanced Research in Virtual and Rapid Prototyping, *Proceedings of the 6th International Conference on Advanced Research in Virtual and Rapid Prototyping*, CRC Press: 149.
33. Bisht G S, Canton G, Mirsepassi A, *et al*., 2011, Controlled continuous patterning of polymeric nanofibers on three-dimensional substrates using low-voltage near-field Electrospinning. *Nano Letters*, vol.11(4): 1831–1837. http://dx.doi.org/10.1021/nl2006164
34. Chang C, Limkrailassiri K and Lin L, 2008, Continuous near-field electrospinning for large area deposition of orderly nanofiber patterns. *Applied Physics Letters*, vol.93(12): 123111. http://dx.doi.org/10.1063/1.2975834
35. Li J L, Guo Y L, Thian E S, *et al*., 2013, 3-Dimensional meniscal fibrillar scaffolds, apparatus and process for the fabrication thereof, UK Patent filing, 2013. Application No. 1315074.3.